A LARGE DEFORMATION AND THERMOMECHANICALLY COUPLED INTERFACE APPROACH

M. KALISKE*, R. FLEISCHHAUER*, R. BEHNKE* AND I. M. ZREID*

*Institute for Structural Analysis
Technische Universität Dresden
01062 Dresden, Germany
e-mail: michael.kaliske@tu-dresden.de

Key words: thermomechanics, interface element, finite deformation

Abstract. Interfaces are formed e.g. by the contact surface of different materials of heterogeneous solids or by crack flanks within damaged bodies. Since the combination of temperature evolution and mechanical loadings influences significantly the deformation and thermal behavior of interfacial layers, these failure layers are thermally and mechanically described in the presented approach in a fully coupled sense. Thermomechanical interface descriptions can be used for prediction of crack propagation and, as soon as a designated failure layer exists, to predict the thermomechanical behavior of the observed solid. The presented interface approach for finite deformation introduces a consistent framework derived from principle thermodynamical laws.

1 INTRODUCTION

Interfacial layers are caused by e.g. the manufacturing process of heterogeneous solids, where they determine a designated failure layer between the different components of such a solid. Also crack flanks in homogeneous bodies determine an interface. In order to predict crack propagation within homogeneous solids or within heterogeneous solids, thermomechanical interface descriptions can be used (see [1]). The presented framework is introduced in a spatial setting of the thermodynamical balance equations. Consequently, the true mechanical and true thermal quantities are constitutively described. Bonds between the opening flanks are the main phenomena of a separation process. The transmission of tractions and heat is constitutively described in terms of elastic and inelastic thermomechanical behavior. The mechanical part of the material description is obtained by considering the equilibrium of forces within the bonds between the interface surfaces, while the thermal part of the constitutive formulations is derived from the balance of thermal energy within the interface. Finally, numerical examples are shown in order to demonstrate the capabilities of the element formulation.

2 KINEMATICS OF INTERFACES

Consider B as the observed solid body having different subbodies B_i, for which $B_i \subset B$ holds. Let $\boldsymbol{\varphi} : B \times \mathscr{R}^3 \to \mathscr{R}^3$ be the nonlinear deformation map of B at material point $\boldsymbol{X} \in B$ and time $t \in \mathscr{R}$. Therewith, $\boldsymbol{\varphi}$ maps points $\boldsymbol{X} \in B$ onto points $\boldsymbol{x} = \boldsymbol{\varphi}(\boldsymbol{X}, t)$. $\boldsymbol{F} := \partial_{\boldsymbol{X}} \boldsymbol{\varphi}(\boldsymbol{X}, t)$ is the deformation gradient with the Jacobian $J := \det[\boldsymbol{F}] > 0$. The velocity field is given with $\dot{\boldsymbol{\varphi}} = \boldsymbol{v} = \partial_t \boldsymbol{\varphi}(\boldsymbol{X}, t)$ and defines the spatial velocity gradient $\boldsymbol{l} := \partial_{\boldsymbol{x}} \dot{\boldsymbol{\varphi}}(\boldsymbol{X}, t)$. In terms of an interface between two subbodies B_i and B_k, the boundaries $\partial B_i \supset \Omega$ and $\partial B_k \supset \Omega$ are piecewise identical along the connective interface $\Omega \subset B$. The opening displacement between two points $(+) \in \Omega$ and $(-) \in \Omega$ can be described by the opening vector $\boldsymbol{\Delta} = \boldsymbol{x}^+ - \boldsymbol{x}^-$, where $\boldsymbol{x}^+ \in B_i$ and $\boldsymbol{x}^- \in B_k$. The related points are initially connected having the same coordinates $\boldsymbol{X}^+ \in B_i$, $\boldsymbol{X}^- \in B_k$ at Ω_{ref}^+ and Ω_{ref}^-. Both points start to seperate as soon as the bonding between them is smaller than its connective forces. The unified kinematics of not separating into tangential and normal directions are firstly introduced in [2].

3 THERMOMECHANICS OF AN INTERFACE AND RELATED FINITE ELEMENT EQUATIONS

In the following section, the continuum balance principles of linear momentum and energy are extended to the interfacial description. The expressions have to be supplemented by additional boundary terms related to Ω.

3.1 Mechanical equlibrium

The balance of linear momentum

$$\rho \dot{\boldsymbol{v}} = \rho \boldsymbol{b} + \mathrm{div}(\boldsymbol{\sigma}) \tag{1}$$

represents the mechanical equilibrium condition of any deformation process. The Galerkin method is applied on its spatial form

$$\int_{\mathcal{B}} \delta \boldsymbol{u} \cdot \mathrm{div}(\boldsymbol{\sigma}) \, dv - \int_{\mathcal{B}} \delta \boldsymbol{u} \cdot (\rho \ddot{\boldsymbol{u}} - \rho \boldsymbol{b}) \, dv = 0 \; , \tag{2}$$

where $\delta \boldsymbol{u}$ is a test function, satisfying $\delta \boldsymbol{u} := \{\delta \boldsymbol{u} \in \mathcal{B}_0 | \delta \boldsymbol{u} = 0 \text{ on } \partial \mathcal{B}_{0_{\boldsymbol{u}}}\}$. Since the Cauchy stresses are symmetric and the divergence theorem $\mathrm{div}(\boldsymbol{\sigma} \delta \boldsymbol{u}) = \mathrm{div}(\boldsymbol{\sigma}) \cdot \delta \boldsymbol{u} + \boldsymbol{\sigma} : \mathrm{grad}(\delta \boldsymbol{u})$ as well as the Gauss theorem holds, one can express Eq. (2) as

$$\int_{\mathcal{B}} \boldsymbol{\sigma} : \mathrm{grad}(\delta \boldsymbol{u}) \, dv - \int_{\partial \mathcal{B}} (\boldsymbol{\sigma} \delta \boldsymbol{u}) \cdot \boldsymbol{n} \, da +$$

$$\int_{\mathcal{B}} \delta \boldsymbol{u} \cdot (\rho \ddot{\boldsymbol{u}} - \rho \boldsymbol{b}) \, dv - \int_{\Omega^+} \delta \boldsymbol{u}^+ \cdot \boldsymbol{t}^+ d\Omega^+ - \int_{\Omega^-} \delta \boldsymbol{u}^- \cdot \boldsymbol{t}^- d\Omega^- = 0 \; . \tag{3}$$

The boundary term of Eq. (3) contains the external tractions $(\boldsymbol{\sigma}\delta\boldsymbol{u})\cdot\boldsymbol{n} = \delta\boldsymbol{u}\cdot(\boldsymbol{\sigma}\boldsymbol{n}) = \delta\boldsymbol{u}\cdot\boldsymbol{t}_e$. Together with the body forces $\boldsymbol{b}$ as well as the inertia term $\rho\ddot{\boldsymbol{u}}$, the external forces are represented. The integrals over Ω^+ and Ω^- are the contributions coming from the opening interface. The test function $\delta\boldsymbol{u}^+$ is defined at Ω^+ and the test function $\delta\boldsymbol{u}^-$ is defined at Ω^-. Subsequently, Eq. (3) has to be discretized, using e.g. linear ansatz functions $\boldsymbol{N}(\boldsymbol{\xi})$ for the shape of the elements, according to the isoparametric concept of the finite element method with local coordinates $\boldsymbol{\xi}$. The displacement field $\boldsymbol{u} = \boldsymbol{x} - \boldsymbol{X}$ is discretized according to $\boldsymbol{u} = \boldsymbol{N}(\boldsymbol{\xi})\boldsymbol{d}^E$, where $\boldsymbol{d}^E$ denotes the nodal displacements of one element. The test function is also discretized by $\delta\boldsymbol{u} = \boldsymbol{N}(\boldsymbol{\xi})\delta\boldsymbol{d}^E$. The gradient of the test function is discretized by $\mathrm{grad}(\boldsymbol{u}) = \partial_{\boldsymbol{x}}\boldsymbol{N}(\boldsymbol{\xi})\boldsymbol{d}^E = \boldsymbol{B}(\boldsymbol{\xi})\boldsymbol{d}^E$. Now, the finite element equations of the discretized equilibrium condition can be formulated

$$
\boldsymbol{G}_M = \mathop{\mathbf{A}}_{E=1}^{N} \left[\int_{\mathcal{B}_E} \boldsymbol{B}^T\boldsymbol{\sigma}\, dv + \left(\int_{\mathcal{B}_E} \boldsymbol{N}^T\rho\boldsymbol{N}\, dv \right) \ddot{\boldsymbol{d}}^E - \int_{\mathcal{B}_E} \boldsymbol{N}^T\left(\rho\boldsymbol{b}\right)\, dv - \int_{\partial\mathcal{B}_E} \boldsymbol{N}^T\boldsymbol{t}_e\, da \right.
$$

$$
\left. - \int_{\Omega_E^+} \boldsymbol{N}_{\Omega^+}^T\boldsymbol{t}^+ d\Omega^+ - \int_{\Omega_E^-} \boldsymbol{N}_{\Omega^-}^T\boldsymbol{t}^- d\Omega^- \right] \tag{4}
$$

$$
= \mathop{\mathbf{A}}_{E=1}^{N} \left[\boldsymbol{f}_{int}^E + \boldsymbol{m}^E\ddot{\boldsymbol{d}}^E - \boldsymbol{f}_{ext}^E - \boldsymbol{f}_{ifc}^E \right] = \boldsymbol{0} \; . \tag{5}
$$

The test function defined at the boundaries Ω^+ and Ω^-, are discretized by

$$
\delta\boldsymbol{u}^+ = \boldsymbol{N}(\xi_1, \xi_2, \xi_3 = +1)\delta\boldsymbol{d}^E \tag{6}
$$

$$
= \boldsymbol{N}_{\Omega^+}\delta\boldsymbol{d}^E \tag{7}
$$

$$
\delta\boldsymbol{u}^- = \boldsymbol{N}(\xi_1, \xi_2, \xi_3 = -1)\delta\boldsymbol{d}^E \tag{8}
$$

$$
= \boldsymbol{N}_{\Omega^-}\delta\boldsymbol{d}^E \; . \tag{9}
$$

3.2 Thermal equilibrium

Before dealing with the thermal equilibrium, an evolution equation for the temperature is needed. This property can be obtained by the following briefly described steps. Starting, the spatial description of dissipation is defined $\rho\gamma\theta \geq 0$. The dissipation has to be additively split into local ($\mathcal{D}_{loc}$) and conductive ($\mathcal{D}_{con}$) parts, $\mathcal{D} = \mathcal{D}_{loc} + \mathcal{D}_{con}$. It is common to require a strict positiveness for both parts. Therefrom, the Clausius-Planck inequality

$$
\mathcal{D}_{loc} := \rho\theta\dot{\eta} - \rho r + \mathrm{div}(\boldsymbol{q}) \geq 0 \; , \tag{10}
$$

is introduced. One can incorporate the spatial energy balance

$$
\rho\dot{e} = \boldsymbol{\sigma} : (\boldsymbol{g}\boldsymbol{l}) + \rho r - \mathrm{div}(\boldsymbol{q}) \tag{11}
$$

into Eq. (10) resulting in

$$\mathcal{D}_{loc} := \rho\theta\dot{\eta} - \rho\dot{e} + \boldsymbol{\sigma} : (\boldsymbol{g}\boldsymbol{l}) \geq 0 \ . \tag{12}$$

Following, the Helmholtz free energy ψ has to be defined through the partial Legendre transformation $\psi := e - \theta\eta$, which implies certain dependencies of the Helmholtz free energy. One can consider a homogeneous inelastic material, where the free energy $\psi = \psi(\boldsymbol{g}, \boldsymbol{F}, \theta, \boldsymbol{\mathcal{G}}, \boldsymbol{\mathcal{I}})$ is a function of the temperature gradient $\boldsymbol{\mathcal{G}}$, the deformation gradient $\boldsymbol{F}$, the absolute temperature θ and a set of internal variables $\boldsymbol{\mathcal{I}}$. The spatial metric $\boldsymbol{g}$ is needed in order to map deformation measures onto the reference configuration. Consequently, the time derivative of the free energy reads

$$\dot{\psi} = \partial_{\boldsymbol{F}}\psi : \dot{\boldsymbol{F}} + \partial_{\theta}\psi \cdot \dot{\theta} + \partial_{\boldsymbol{\mathcal{I}}}\psi : \dot{\boldsymbol{\mathcal{I}}} + \partial_{\boldsymbol{\mathcal{G}}}\psi : \dot{\boldsymbol{\mathcal{G}}} \ . \tag{13}$$

Using the Legendre transformation, the time derivative of the internal energy yields the form

$$\dot{e} := \dot{\psi} + \dot{\theta}\eta + \theta\dot{\eta} \ . \tag{14}$$

Incorporating Eq. (14) into Eq. (12) results in

$$\boldsymbol{\sigma} : (\boldsymbol{g}\boldsymbol{l}) - \rho\dot{\psi} - \rho\eta\dot{\theta} \geq 0 \ . \tag{15}$$

Next, the time derivative of the free energy (Eq. (13)) has to be plugged into Eq. (15). Using the definition of the spatial velocity gradient $\boldsymbol{l} = \dot{\boldsymbol{F}}\boldsymbol{F}^{-1}$ and the conservation of mass, $J \cdot \rho = \rho_0$ as well as the relation between Cauchy and first Piola-Kirchhoff stress, $\boldsymbol{\sigma} = 1/J \cdot \boldsymbol{P}\boldsymbol{F}^T$, the resulting thermodynamic restriction is defined as

$$[\boldsymbol{g}\boldsymbol{P} - \rho_0\partial_{\boldsymbol{F}}\psi] : \dot{\boldsymbol{F}} - \rho_0[\eta + \partial_{\theta}\psi] \cdot \dot{\theta} - \rho_0[\partial_{\boldsymbol{\mathcal{G}}}\psi] : \dot{\boldsymbol{\mathcal{G}}} - \rho_0[\partial_{\boldsymbol{\mathcal{I}}}\psi] : \dot{\boldsymbol{\mathcal{I}}} \geq 0 \ . \tag{16}$$

Following [3, 4], the thermodynamic restriction should be fulfilled for an arbitrary rate of deformation gradient, temperature and temperature gradient, which yields in Eq. (16),

$$\rho_0\partial_{\boldsymbol{F}}\psi = \boldsymbol{g}\boldsymbol{P} \ , \tag{17}$$

$$\eta = -\partial_{\theta}\psi \ , \tag{18}$$

$$\partial_{\boldsymbol{\mathcal{G}}}\psi = \boldsymbol{0} \ . \tag{19}$$

Considerung Eqs. (17), (18) and (19), Eq. (10) reduces to

$$\mathcal{D}_{loc} := -\rho_0\partial_{\boldsymbol{\mathcal{I}}}\psi : \dot{\boldsymbol{\mathcal{I}}} \geq 0 \ . \tag{20}$$

Furthermore, inserting Eq. (13) into Eq. (14) reads

$$\dot{e} = \partial_{\boldsymbol{F}}\psi : \dot{\boldsymbol{F}} + \partial_{\theta}\psi \cdot \dot{\theta} + \underbrace{\partial_{\boldsymbol{\mathcal{G}}}\psi}_{=0} : \dot{\boldsymbol{\mathcal{G}}} + \partial_{\boldsymbol{\mathcal{I}}}\psi : \dot{\boldsymbol{\mathcal{I}}} + \eta\dot{\theta} + \theta\dot{\eta} \ . \tag{21}$$

Inserting this expression into the balance of energy, under the use of Eqs. (17), (18) and (19), the balance of entropy equation

$$\rho\theta\dot{\eta} = -\rho \cdot [\partial_{\mathcal{I}}\psi] : \dot{\mathcal{I}} + \rho r - \operatorname{div} \boldsymbol{q} \tag{22}$$

is obtained. The last step is the insertion of the rate of entropy

$$\dot{\eta} = -\partial_{\theta\theta}^2\psi \cdot \dot{\theta} - \partial_{\boldsymbol{F}\theta}^2\psi : \dot{\boldsymbol{F}} - \partial_{\mathcal{I}\theta}^2\psi : \dot{\mathcal{I}} \tag{23}$$

into Eq. (22). Under consideration that the heat capacity is defined as $c = -\theta \cdot \partial_{\theta\theta}^2\psi$, the transient heat conduction equation

$$\rho c\dot{\theta} = -\operatorname{div}(\boldsymbol{q}) + \rho r + \underbrace{\rho \cdot [\theta \cdot \partial_{\boldsymbol{F}\theta}^2\psi] : \dot{\boldsymbol{F}}}_{w_{\text{ext}}} - \underbrace{\rho \cdot [\partial_{\mathcal{I}}\psi - \theta \cdot \partial_{\mathcal{I}\theta}^2\psi] : \dot{\mathcal{I}}}_{w_{\text{int}}} \tag{24}$$

is formulated. Furthermore, one has to apply the Galerkin method to the transient heat conduction equation in order to achieve the finite element equations. Therefore, Eq. (24) is multiplied with an arbitrary test function $\delta\theta$ satisfying $\delta\theta := \{\delta\theta \in \mathcal{B}_0 | \delta\theta = 0 \text{ on } \partial\mathcal{B}_{0\theta}\}$. The integration over the current volume yields

$$\int_{\mathcal{B}} \delta\theta\rho c\dot{\theta}\, dv - \int_{\mathcal{B}} \delta\theta\rho r\, dv + \int_{\mathcal{B}} \delta\theta \operatorname{div}(\boldsymbol{q})\, dv - \int_{\mathcal{B}} \delta\theta w_{\text{ext}}\, dv + \int_{\mathcal{B}} \delta\theta w_{\text{int}}\, dv = 0 \ . \tag{25}$$

The divergence theorem $(\delta\theta \operatorname{div}(\boldsymbol{q})) = (\operatorname{div}(\delta\theta\boldsymbol{q})) - (\operatorname{grad}(\delta\theta) \cdot \boldsymbol{q})$ can be applied and, together with the Gauss theorem, results in

$$\int_{\mathcal{B}} \delta\theta\rho c\dot{\theta}\, dv - \int_{\mathcal{B}} \delta\theta\rho r\, dv + \int_{\partial\mathcal{B}} \delta\theta \cdot (\boldsymbol{q} \cdot \boldsymbol{n})\, da - \int_{\mathcal{B}} \operatorname{grad}(\delta\theta) \cdot \boldsymbol{q}\, dv - \int_{\mathcal{B}} \delta\theta \cdot w_{\text{ext}}\, dv +$$

$$\int_{\mathcal{B}} \delta\theta \cdot w_{\text{int}}\, dv + \int_{\Omega^+} \delta\theta^+ \cdot (\boldsymbol{q}^+ \cdot \boldsymbol{n}^+ - w^+)d\Omega^+ + \int_{\Omega^-} \delta\theta^- \cdot (\boldsymbol{q}^- \cdot \boldsymbol{n}^- - w^-)d\Omega^- = 0 \ . \tag{26}$$

The external thermal conduction energy $(\boldsymbol{q} \cdot \boldsymbol{n}) = h_e$ is identified as the boundary term. The additional contributions at the boundaries Ω^+ and Ω^- have to be considered, since they are caused by the opening crack flanks. The thermal conduction energies $h^+ = (\boldsymbol{q}^+ \cdot \boldsymbol{n}^+)$ and $h^- = (\boldsymbol{q}^- \cdot \boldsymbol{n}^-)$, as well as the power terms $w^+ = w_{ext}^+ - w_{int}^+$ and $w^- = w_{ext}^- - w_{int}^-$ describe the energy of the surfaces Ω^+ and Ω^-, since they are originated in heat flux and power terms of the bonds between the opening flanks. Furthermore, the temperature field is discretized as $\theta = \boldsymbol{N}_\theta(\boldsymbol{\xi})\boldsymbol{\theta}^E$, as well as the test function $\delta\theta = \boldsymbol{N}_\theta(\boldsymbol{\xi})\delta\boldsymbol{\theta}^E$. The test function defined at the boundaries Ω^+ and Ω^-, are discretized by

$$\delta\theta^+ = \boldsymbol{N}_\theta(\xi_1, \xi_2, \xi_3 = +1)\delta\boldsymbol{\theta}^E \tag{27}$$

$$= \boldsymbol{N}_{\theta\Omega^+}\delta\boldsymbol{\theta}^E \tag{28}$$

$$\delta\theta^- = \boldsymbol{N}_\theta(\xi_1, \xi_2, \xi_3 = -1)\delta\boldsymbol{\theta}^E \ , \tag{29}$$

$$= \boldsymbol{N}_{\theta\Omega^-}\delta\boldsymbol{\theta}^E \ . \tag{30}$$

(a) Equilibrium of forces
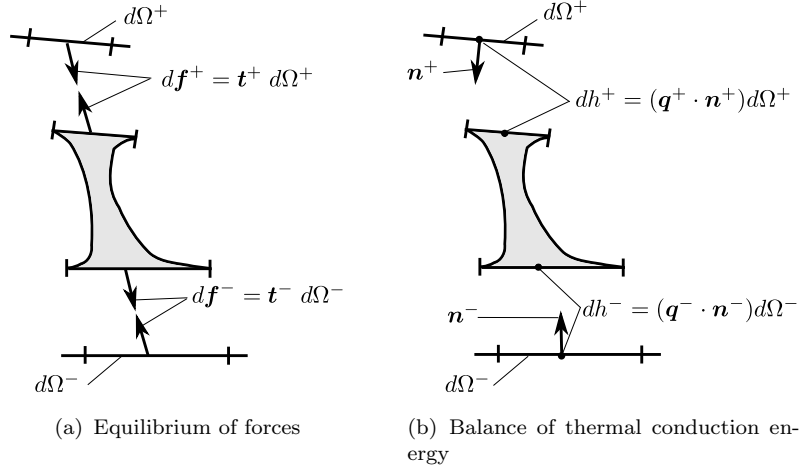
(b) Balance of thermal conduction energy

Figure 1: Schematical description of a bond of an opened interface element

Finally, one can formulate the finite element equations of the thermal equilibrium

$$
\boldsymbol{G}_T = \mathop{\mathbf{A}}_{E=1}^{N} \left[\int_{\mathcal{B}_E} \boldsymbol{N}_\theta^T \rho c \dot{\theta} \, dv - \int_{\mathcal{B}_E} \boldsymbol{N}_\theta^T r \, dv + \int_{\partial \mathcal{B}_E} \boldsymbol{N}_\theta^T h_e \, da \right.
$$

$$
- \int_{\mathcal{B}_E} \boldsymbol{B}_\theta^T \boldsymbol{q} \, dv - \int_{\mathcal{B}_E} \boldsymbol{N}_\theta^T w_{\text{ext}} \, dv + \int_{\mathcal{B}_E} \boldsymbol{N}_\theta^T w_{\text{int}} \, dv
$$

$$
\left. + \int_{\Omega_E^+} \boldsymbol{N}_{\theta \Omega^+}^T (\boldsymbol{q}^+ \cdot \boldsymbol{n}^+ - w^+) d\Omega^+ + \int_{\Omega_E^-} \boldsymbol{N}_{\theta \Omega^-}^T (\boldsymbol{q}^- \cdot \boldsymbol{n}^- - w^-) d\Omega^- \right] = \boldsymbol{0} \; . \qquad (31)
$$

4 THERMAL ENERGY AND TRACTION-SEPARATION-LAW (TSL)

After having derived the finite element equations, the constitutive descriptions of an interface can be defined. The main mechanism of debonding is the development of connective bonds between opening interface surfaces as depicted in Fig. 1. In order to have equilibrium of forces (see Fig. 1(a)) within the interface element, $\boldsymbol{t}^+ := -\boldsymbol{t} \cdot J_A^+$ and $\boldsymbol{t}^- := +\boldsymbol{t} \cdot J_A^-$ are introduced. The traction quantities $\boldsymbol{t}^+$ and $\boldsymbol{t}^-$ can have different values on the opposite surfaces Ω^+ and Ω^-, since in general different changes of the area of these surfaces are allowed. This is achieved by scaling the current tractions $\boldsymbol{t}$ according to the change of their related differential area. The area change is described by $J_A^+ = d\Omega_{ref}^+/d\Omega^+$ and $J_A^- = d\Omega_{ref}^-/d\Omega^-$ and can be generally determined from the area map $\boldsymbol{n} \, da = J \boldsymbol{F}^{-T} \boldsymbol{N} \, dA$ and the current normal definition $\boldsymbol{n} = \boldsymbol{F}^{-T} \boldsymbol{N}$, that leads to the

expressions

$$\boldsymbol{n}\, da = J \boldsymbol{F}^{-T} \boldsymbol{N}\, dA = J \boldsymbol{n}\, dA \;, \tag{32}$$

$$J_A = \frac{dA}{da} = \frac{1}{J} \;. \tag{33}$$

Therewith, the condition for the equilibrium of forces

$$\boldsymbol{f}^+ = -\,\boldsymbol{f}^- \;, \tag{34}$$

$$\int_{\Omega^+} \boldsymbol{t}^+ d\Omega^+ = \int_{\Omega^-} \boldsymbol{t}^- d\Omega^- \tag{35}$$

is fulfilled for the same initial area Ω_{ref} of both surfaces. It is possible to think of the current traction vectors $\boldsymbol{t}^+$ and $\boldsymbol{t}^-$ as Cauchy tractions at the crack surfaces, while the transformation with J_A^+ and J_A^- results in Kirchhoff tractions $+\boldsymbol{t}$ and $-\boldsymbol{t}$. This transformation yields a change of the integration areas, while evaluating the reaction forces at the ends of a delamination bond (compare Fig. 1(a)).

Considering an opened crack within the observed body B, the crack surfaces as well as the bonds between them undergo different thermal conduction and convection mechanisms, respectively. The thermal convection at the crack surfaces, that transfers heat between the subbodies B_i and the surrounding environment is not considered in the proposed element formulation. The thermal conduction through the connective bonds between the crack surfaces is denoted by a zero sum of the total heat in- and outflux of the Ω^+ and the Ω^- surfaces, due to a zero loss or gain of thermal heat flux energy on an interface element. Therefore, the balance of thermal conduction energy (see Fig. 1(b)) is obtained according to

$$h^+ = -\,h^- \;, \tag{36}$$

$$\int_{\Omega^+} \left(\boldsymbol{q}^+ \cdot \boldsymbol{n}^+ \right) d\Omega^+ = \int_{\Omega^-} \left(\boldsymbol{q}^- \cdot \boldsymbol{n}^- \right) d\Omega^- \;. \tag{37}$$

The balance condition in Eq. (37) can be fulfilled for $(\boldsymbol{q} \cdot \boldsymbol{n})^+ := -(\boldsymbol{q} \cdot \boldsymbol{n}) \cdot J_A^+$ and $(\boldsymbol{q} \cdot \boldsymbol{n})^- := (\boldsymbol{q} \cdot \boldsymbol{n}) \cdot J_A^-$. Similiar to the traction quantities $\boldsymbol{t}^+$ and $\boldsymbol{t}^-$, the thermal conduction quantities $(\boldsymbol{q} \cdot \boldsymbol{n})^+$ and $(\boldsymbol{q} \cdot \boldsymbol{n})^-$ are spatial objects. The constitutive descriptions of the introduced quantitties $\boldsymbol{t}^+$, $\boldsymbol{t}^-$ and $(\boldsymbol{q} \cdot \boldsymbol{n})^+$, $(\boldsymbol{q} \cdot \boldsymbol{n})^-$ are given in the following subsections.

4.1 Traction-separation-laws

The tractions are defined as $\boldsymbol{t}^+ := -\boldsymbol{t} \cdot J_A^+$ and $\boldsymbol{t}^- := +\boldsymbol{t} \cdot J_A^-$. The relation between the spatial tractions $\boldsymbol{t}$ and current separation $\boldsymbol{\Delta}$ can be obtained from a TSL-potential.

4.1.1 Elastic TSL-potential

The proposed elastic potential is an extension of the one in [5] and it is defined per unit reference area. The specific form of the proposed potential reads

$$\Phi(\boldsymbol{\Delta}, [\![\theta]\!]) := \phi - \frac{\phi}{\delta}(\|\boldsymbol{\Delta}\| + \delta) \exp\left(-\frac{\|\boldsymbol{\Delta}\|}{\delta}\right) - \frac{1}{2}\alpha_t \frac{\phi}{\delta^2}[\![\theta]\!]\|\boldsymbol{\Delta}\|^2 \ , \tag{38}$$

where ϕ is a material parameter, representing the work or energy of separation, δ is a characteristic opening length and α_t is the thermal expansion coefficient. To derive the TSL, the derivative $\partial_{\boldsymbol{\Delta}}\Phi(\boldsymbol{\Delta}, [\![\theta]\!])$ is needed. In case of Eq. (38), it reads

$$\boldsymbol{t}(\boldsymbol{\Delta}, [\![\theta]\!]) = \partial_{\boldsymbol{\Delta}}\Phi(\boldsymbol{\Delta}, [\![\theta]\!]) = \frac{\phi}{\delta^2} \exp\left(-\frac{\|\boldsymbol{\Delta}\|}{\delta}\right)\boldsymbol{\Delta} - \alpha_t \frac{\phi}{\delta^2}[\![\theta]\!]\boldsymbol{\Delta} \ . \tag{39}$$

4.1.2 Inelastic TSL-potential

The inelastic traction separation law is derived from a viscoelastic potential $\Phi = \Phi^e(\theta, \boldsymbol{\Delta}) + \Phi^v(\theta, \boldsymbol{\Delta}, \boldsymbol{\Delta}^v)$, that consists of an elastic Φ^e part and a viscous Φ^v part. The total separation $\boldsymbol{\Delta} = \boldsymbol{\Delta}^e + \boldsymbol{\Delta}^v$ is split into an elastic and a viscous part. Consequently, the total tractions are determined by an addition of the elastic and viscous tractions, $\boldsymbol{t} = \boldsymbol{t}^e + \boldsymbol{t}^v$. The elastic part $\Phi^e(\theta, \boldsymbol{\Delta})$ of the TSL potential reads

$$\Phi^e(\boldsymbol{\Delta}, \theta) = \phi - \frac{\phi}{\delta}(\|\boldsymbol{\Delta}\| + \delta) \exp\left(-\frac{\|\boldsymbol{\Delta}\|}{\delta}\right) \exp\left(\frac{-\vartheta}{\theta_b}\right) \ . \tag{40}$$

Similar to Eq. (38), ϕ denotes the work of separation and δ is the characteristic opening length. The change of the temperature $\vartheta = \theta_r - \theta$ relative to the reference temperature θ_r at the middle of the interface is related to characteristic temperature θ_b at the middle of the interface. The viscous part of the inelastic TSL is given as

$$\Phi^v(\boldsymbol{\Delta}, \boldsymbol{\Delta}^v, \theta) = \frac{1}{2}\beta\frac{\phi}{\delta^2} \exp\left(-\frac{\|\boldsymbol{\Delta}\|}{\delta}\right) \exp\left(\frac{-\vartheta}{\theta_b}\right)\|\boldsymbol{\Delta} - \boldsymbol{\Delta}^v\|^2 \ , \tag{41}$$

where β is a material parameter representing the relation between the elastic and the viscous part of the work of separation. The elastic tractions can be derived from the elastic part of Φ and read

$$\boldsymbol{t}^e(\boldsymbol{\Delta}, \theta) = \frac{\partial}{\partial\boldsymbol{\Delta}}\Phi^e = \frac{\phi}{\delta^2} \exp\left(-\frac{\|\boldsymbol{\Delta}\|}{\delta}\right) \exp\left(\frac{-\vartheta}{\theta_b}\right)\boldsymbol{\Delta} \ , \tag{42}$$

while the viscous tractions are given as

$$\boldsymbol{t}^v(\boldsymbol{\Delta}, \boldsymbol{\Delta}^v, \theta) = -\frac{\partial}{\partial\boldsymbol{\Delta}^v}\Phi^v = \beta\frac{\phi}{\delta^2} \exp\left(-\frac{\|\boldsymbol{\Delta}\|}{\delta}\right) \exp\left(\frac{-\vartheta}{\theta_b}\right)(\boldsymbol{\Delta} - \boldsymbol{\Delta}^v) \ . \tag{43}$$

The motivation for the chosen viscous potential and the resulting tractions is, to achieve the viscous tractions as a function of the elastic tractions. It can be seen that

$$\boldsymbol{t}^v = \beta \left\| \boldsymbol{t}^e \right\| \frac{(\boldsymbol{\Delta} - \boldsymbol{\Delta}^v)}{\left\| \boldsymbol{\Delta} \right\|} \ . \tag{44}$$

The characteristic length δ is calculated from the material parameters, according to

$$\delta = \frac{\phi \cdot \exp \left(\frac{-\vartheta}{\theta_b} \right)}{T_{max} \cdot \exp \left(1 \right)} \ . \tag{45}$$

The evolution law for the viscous part of the separation reads

$$\dot{\boldsymbol{\Delta}}^v = \frac{\delta_v}{\eta} \boldsymbol{t}^v \ , \tag{46}$$

where η is the viscosity and the characteristic length δ_v for the viscous part is determined by

$$\delta_v = \beta \delta. \tag{47}$$

The viscosity is temperature dependent and may be described by Williams-Landel-Ferry equation

$$\eta = \eta_0 \left(\frac{-C_1 \left(\theta - \theta_r \right)}{C_2 + \theta + \theta_r} \right) \ , \tag{48}$$

where η_0 is the viscosity at the reference temperature and C_1 and C_2 are additional material parameters.

4.2 Thermal conduction energy and rate of work

As stated in Eq. (37), $(\boldsymbol{q} \cdot \boldsymbol{n})^+$ and $(\boldsymbol{q} \cdot \boldsymbol{n})^-$ have to be expressed. Additionally, the rate of work done by the tractions at the Ω^+ and Ω^- surfaces is derived. The proposed formulations of the thermal conduction energy per unit reference areas are given by

$$(\boldsymbol{q} \cdot \boldsymbol{n})^+ := - \left(\boldsymbol{q} \cdot \boldsymbol{n} \right) \cdot J_A^+ = - \left(-k \frac{[\![\theta]\!]}{\left\| \boldsymbol{\Delta} \right\|} \right) \cdot J_A^+ \ , \tag{49}$$

$$(\boldsymbol{q} \cdot \boldsymbol{n})^- := \left(\boldsymbol{q} \cdot \boldsymbol{n} \right) \cdot J_A^- = \left(-k \frac{[\![\theta]\!]}{\left\| \boldsymbol{\Delta} \right\|} \right) \cdot J_A^- \ . \tag{50}$$

One can assume that the heat is mainly transferred along the connective bonds, as soon as the separation process between the two materials has started $\left\| \boldsymbol{\Delta} \right\| > 0$ and as soon as a difference between the temperatures of both sides $[\![\theta]\!] = \theta^+ - \theta^-$ at the initially connected points is found. The introduced formulations of Eq. (49) and Eq. (50) are phenomenological descriptions. The computation of the derivatives $\partial_{[\![\theta]\!]}(\boldsymbol{q} \cdot \boldsymbol{n})$ and $\partial_{\boldsymbol{\Delta}}(\boldsymbol{q} \cdot \boldsymbol{n})$

are required for the incorporation of the element formulation into a FE-framework and are given as

$$\partial_{\boldsymbol{\Delta}}(\boldsymbol{q} \cdot \boldsymbol{n}) = \left(k[\![\theta]\!] \frac{\boldsymbol{\Delta}}{\|\boldsymbol{\Delta}\|^3} \right) \,, \tag{51}$$

$$\partial_{[\![\theta]\!]}(\boldsymbol{q} \cdot \boldsymbol{n}) = \left(-k \frac{1}{\|\boldsymbol{\Delta}\|} \right) \,. \tag{52}$$

The total rates of work $w^+ = w_{ext}^+ - w_{int}^+$ and $w^- = w_{ext}^- - w_{int}^-$ at the opposite flanks of the interface are the result of the subtraction of the internal power from the external power (compare Eq. (24)). Their specific form in terms of the elastic TSL potential reads

$$w^+ := \frac{1}{2} w^{ifc} J_A^+ = \frac{1}{2} [\![\theta]\!] \left[\partial_{[\![\theta]\!]} \boldsymbol{t} \right] \cdot \dot{\boldsymbol{\Delta}} \, J_A^+ \,, \tag{53}$$

$$w^- := \frac{1}{2} w^{ifc} J_A^- = \frac{1}{2} [\![\theta]\!] \left[\partial_{[\![\theta]\!]} \boldsymbol{t} \right] \cdot \dot{\boldsymbol{\Delta}} \, J_A^- \tag{54}$$

and is assigned equally with the coefficient $1/2$ to the sides Ω^+ and Ω^- in a phenomenological way. The contributions of the rates of work in terms of the viscoelastic TSL potential are given as

$$w^+ := \frac{1}{2} \vartheta \left[\partial_{\vartheta \boldsymbol{\Delta}}^2 \Phi \right] \cdot \dot{\boldsymbol{\Delta}} \, J_A^+ - \frac{1}{2} \left[\partial_{\boldsymbol{\Delta}^v} \Phi^v - \partial_{\vartheta \boldsymbol{\Delta}^v}^2 \Phi^v \right] \cdot \dot{\boldsymbol{\Delta}}^v \, J_A^+ \,, \tag{55}$$

$$w^- := \frac{1}{2} \vartheta \left[\partial_{\vartheta \boldsymbol{\Delta}}^2 \Phi \right] \cdot \dot{\boldsymbol{\Delta}} \, J_A^- - \frac{1}{2} \left[\partial_{\boldsymbol{\Delta}^v} \Phi^v - \partial_{\vartheta \boldsymbol{\Delta}^v}^2 \Phi^v \right] \cdot \dot{\boldsymbol{\Delta}}^v \, J_A^- \,. \tag{56}$$

5 NUMERICAL EXAMPLES

Subsequently, two numerical model problems are given for the verification of the proposed element formulation.

5.1 Thermal conduction

The first example is a pure thermal conduction simulation, where the top surface is loaded with a constant temperature rate of $\dot{\theta}_e = 1.5$ K/s for a time of 100 s and, subsequently, the temperature is kept constant for the next 300 s. At the bottom, the thermal boundary condition is a free surface. The solid elements are thermomechanical linear elements. The geometry of 10x10x20 mm is discretized with 128 solid elements and 16 of the proposed thermomechanical elastic interface elements at the middle of the height of the specimen. The mechanical boundary conditions are set such that a stress free state is ensured. The results of the computation containing interface elements are illustrated in Fig. 2, where Fig. 2(a), Fig. 2(b) and Fig. 2(c) contain the graphical illustration of the change in the temperature field at three different times for the computation with the proposed thermoelastic interface elements. Interpreting the obtained results, it is concluded, that the thermal conductivity behavior of the elastic interface element is expressed in a correct manner.
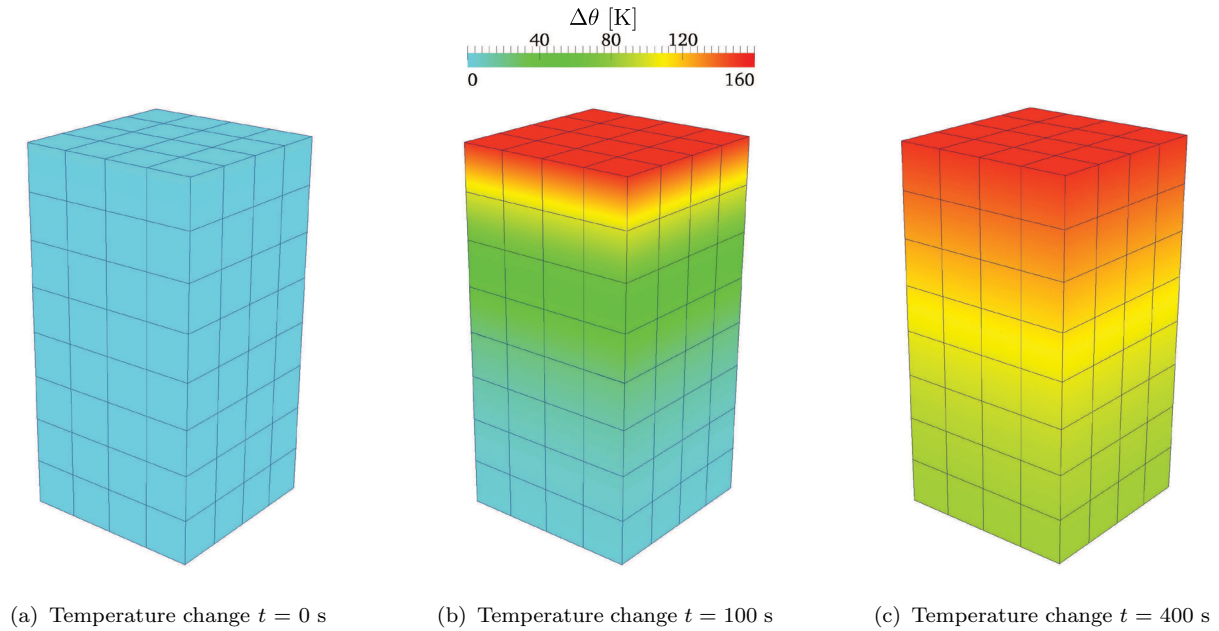
(a) Temperature change $t = 0$ s   (b) Temperature change $t = 100$ s   (c) Temperature change $t = 400$ s

Figure 2: Illustration of thermal conduction simulation

5.2 Predictive tensile simulation

The second example is a tensile test simulation. The geometry of the specimen of 10x10x20 mm is discretized with 54 thermomechanical linear solid elements containing thermoelastic Neo-Hooke material. In the middle of the height of the specimen 9 thermoviscoelastic interface elements are placed. The bottom surface is totally fixed, while a constant rate of displacment of 0.16 mm/s is applied to the top surface for 25 s and afterwards held constant for 75 s. The resulting stress relaxation behavior is depicted in Fig. 3, where the initial stress free configuration is depicted in Fig. 3(a), the maximum stress situation is shown in Fig. 3(b) and relaxation of stress can be seen from Fig. 3(c). The stress relaxation within the interface generates an increase in the opening of the interface. Therefrom, a physically correct behavior of the proposed element and constitutive formulation is concluded.

6 CONCLUSIONS

- A thermomechanically coupled interface element formulation in the spatial setting is introduced.

- Elastic and inelastic thermomechanical TSL-potentials for deriving tractions and internal, as well as external work terms are introduced.

- Numerical examples are shown in order to demonstrate the potential capabilities of the proposed formulations.
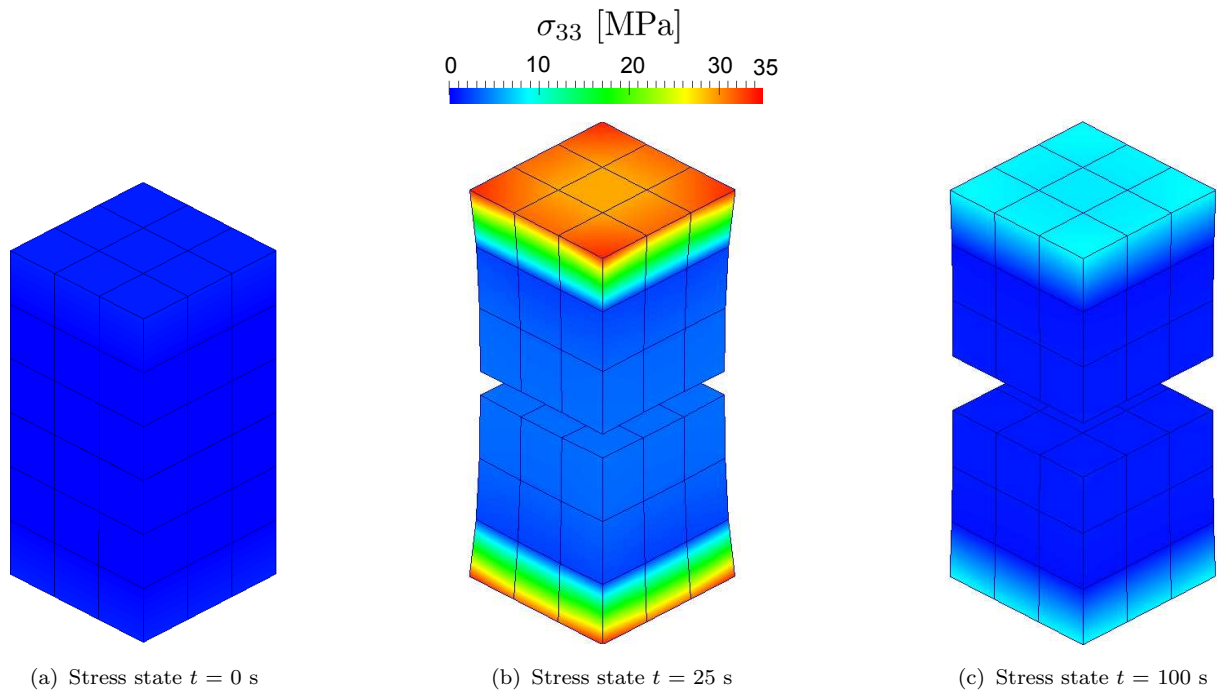
σ_{33} [MPa]

(a) Stress state $t = 0$ s   (b) Stress state $t = 25$ s   (c) Stress state $t = 100$ s

Figure 3: Illustration of predictive tensile test simulation

REFERENCES

[1] Fleischhauer, R., Behnke, R. and Kaliske, M. A thermomechanical interface element formulation for finite deformations. *Comput Mech* (2013) DOI 10.1007/s00466-013-0862-7.

[2] van den Bosch, M.J., Schreurs, P.J.G. and Geers, M.G.D. A cohesive zone model with large displacement formulation for interfacial fibrilation. *Eur J Mech A-Solid* (2007) **26**:1–19.

[3] Coleman, B. and Gurtin, M.E. Thermodynamics with internal state variables. *J Chem Phys* (1967) **47**:597–613.

[4] Coleman, B. and Noll, W. The thermodynamics of elastic materials with heat conduction and viscosity. *Arch Ration Mech An* (1963) **13**:167–178.

[5] van den Bosch, M.J., Schreurs, P.J.G. and Geers, M.G.D. On the development of a 3D cohesive zone element in the presence of large deformations. *Comput Mech* (2008) **42**:171–180.